

Earthquake-resilient Tall Buildings Using Rocking Walls

Y. Zhou

*State Key Laboratory of Disaster Reduction in Civil Engineering, Tongji University,
Shanghai, China*

R. Li

*Research Institute of Structural Engineering and Disaster Reduction, Tongji University,
Shanghai, China*

X.L. Lu

*State Key Laboratory of Disaster Reduction in Civil Engineering, Tongji University,
Shanghai, China*



SUMMARY:

In this paper, rocking walls were introduced to a 240-meter-high tall building to realize the structural earthquake resilience. The structural system is composed of central reinforced concrete (RC) core walls and peripheral steel reinforced concrete (SRC) frames. Three structures were analytically compared including one with traditional walls, one with rocking walls, and one with rocking walls and additional viscous dampers. Time history analysis with peak ground accelerations of 0.07g, 0.20g, and 0.40g was performed to compare the seismic responses of three structures. It is found that for the latter two rocking systems, the fundamental period is increased by 2 s and the inter-story drift is increased by 30%. The walls are uplifted while the wall compressive stress could be effectively reduced by 30%. It is also noted that, compared to the traditional structure, the bending moment shared by frames of two rocking structures is increased by 30%. The existence of viscous dampers does not affect the internal forces but shorten the vibration duration approximate to the traditional structure. Further studies on global/local deformation and limitations, additional damping ratio, and structural details are still needed for the application of rocking walls in tall buildings.

Keywords: tall building, earthquake resilience, rocking structure, viscous damper

1. INTRODUCTION AND BUILDING INFORMATION

Extensive attention has been recently given to earthquake resilience of building structures in earthquake engineering. Early in 1963, the uplift effect of structure under earthquake action which can mitigate the earthquake damage had firstly noticed by Housener (Housener, 1963). From then on, researchers have done a lot of attempts, such as Huckelbridge and Clough conducted shaking table tests on a 3-storey and 9-storey rocking steel frame structure, respectively (Huckelbridge & Clough, 1977; Huckelbridge, 1977). In 1978, Priestley *et al.* conducted a shaking table test on a rocking structure to prove the energy dissipation mechanism of the rocking structure (Priestley, 1978). In 2000, after a series of test, Kurama developed a kind of self-centering shear wall which has good performance under earthquake action (Kurama, 1996). In 2008, based on the current study on rocking coupled shear wall, Hitaka and Sakino put forward a new coupled shear wall system and conducted static experiment on its performance (Hitaka & Sakino, 2008). In January 2009, the new concept of resilient city had been proposed during the Seventh Joint Planning Meeting of NEES/E-defense Collaborative Research on Earthquake Engineering (PEER, 2010). Nielsen *et al.* studied the seismic performance of the rocking core walls (Nielsen, 2010). To realize structural earthquake resilience without major damages, innovative systems which include rocking structures, self-centering structures, and replaceable structural members are proposed and increasingly studied (Zhou & Lu, 2011).

In this paper, a 240-meter-high tall building was studied, in order to compare the seismic responses of structural systems with different earthquake-resilient measures. Three analytical models were considered including one traditional structure which has fixed-base reinforced concrete walls (Structure A), one rocking structure which has rocking walls (Structure B), and one damped rocking structure with both rocking walls and additional viscous dampers (Structure C).

1.1. Structure A

Structure A has 60 stories with a total height of 240 m. The dimension of the model is 40 m by 40 m, as shown in Fig. 1. The structure is composed of central reinforced concrete (RC) core walls and peripheral steel reinforced concrete (SRC) frames. C60 concrete is used for both SRC columns and core walls; C35 concrete is for slabs; and Q345 steel is applied for the steel of SRC columns and steel beams. The dimensions of the major structural members are listed in Table 1. The analytical model is established using ETABS shown in Fig. 2.

The dead and live load of the building is 5 kN/m² and 2 kN/m², respectively. The seismic fortification intensity of the building site is assumed to be 8, which has a peak ground motion of 0.07g, 0.2g, and 0.4g under minor, moderate, and major earthquake levels, respectively. The seismic site design is Group I and the soil classification is III, which means that the characteristic period is 0.45 s. The wind pressure is 0.66 kN/m².

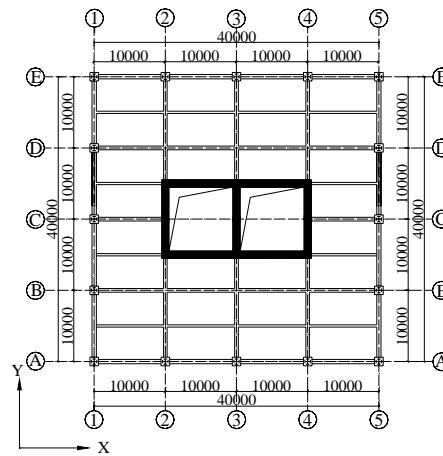

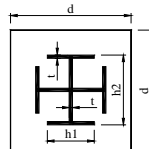
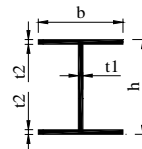


Figure 1. Structure plan layout

Table 1. Dimensions of shear wall and column (mm)

Storey	Shear wall	Column		Beam			Slab
		RC section: d SRC section: h1×h2×t 		Peripheral beam	Central beam	Secondary beam	
		b×h×t1×t2 					
51-60	350	600	300×400×20	500×800×20×40	500×800×20×40	300×500×14×25	120
46-50	500						
41-45		800	400×500×20				
36-40							
31-35	600	1000	500×700×35	500×900×20×40	500×800×20×40	300×500×14×25	
26-30							
21-25	800						
16-20							
11-15	1000	1200	600×900×35	600×950×20×40			
1-10							

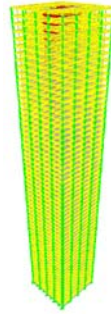


Figure 2. 3-D analytical model of the structure

1.2. Structure B

The structural configuration and member dimensions of Structure B are the same as those of Structure A. The difference between the two structures lies in the boundary condition of the bottom. Structure A has a fixed base with all degrees of freedom restrained at the bottom of the core wall (Fig. 3), while Structure B has only one fixed-base support at the bottom to make the system rock (Fig. 4).

1.3. Structure C

Based on Structure B, ten viscous dampers are attached to the model as Structure C. The dampers are installed in the first floor with one end supported on the basement, the other end connected with a cantilever beam at the height of 3.2 m. The damping coefficient C of the damper is set as $250\text{kN}\cdot\text{s}/\text{mm}$; and the damping exponent α is set as 0.1. The configuration of the cantilever beam and the dampers is shown in Fig. 5.

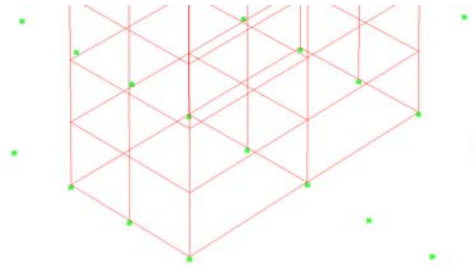


Figure 3. Supports of Structure A

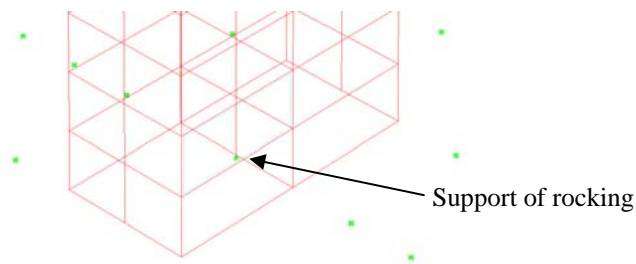


Figure 4. Supports of Structure B

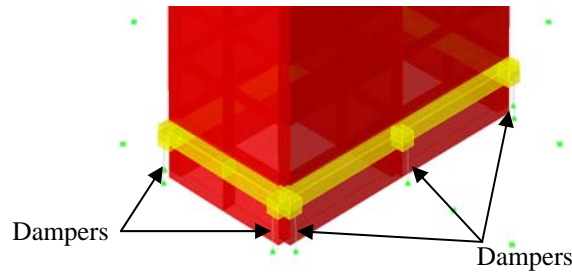


Figure 5. Configurations of viscous dampers and cantilever beam of Structure C

2. DYNAMIC CHARATERISTICS

The first 30 modes were calculated and the corresponding the sum of the modal participating mass ratio exceeds 90% which meet the requirement of *Technical Specification for Concrete Structures of Tall Building* (Ministry of Housing and Urban Rural Development. 2010). The first 9 vibration periods of structures are listed in Table 2. It is found that the vibration modes and periods of Structure B and C are all the same. It can be explained that the viscous damper is a kind of velocity-dependent damper and would not affect the dynamic property of the structures. Compared with Structure A, the first periods are increased by 2 s (35%) and 2.6 s (59%) in Y and X direction, respectively. However, the first and second torsional periods are 1.68 s and 0.65 s, respectively, for all three structures. That is to say, the rocking weaken the translational stiffness while do not change the torsional stiffness of the structures.

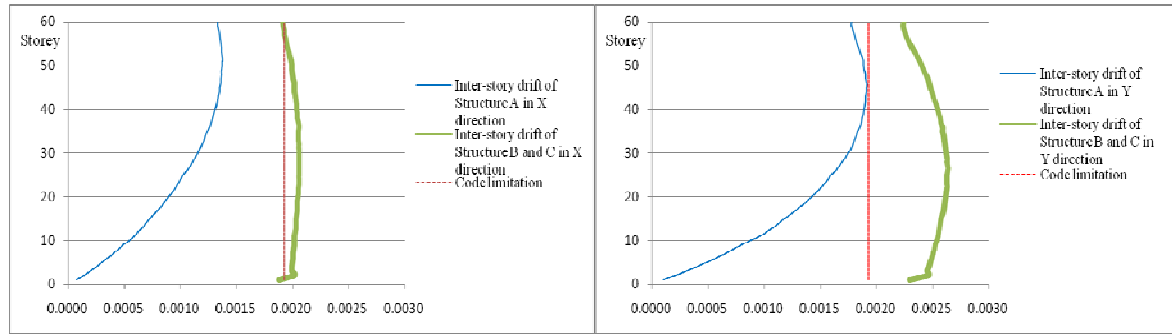
Table 2. Vibration periods of different structures (unit: s)

Modes	Structure A (modal direction)	Structure B (modal direction)	Structure C (modal direction)
1	5.79 (Y)	7.82 (Y)	7.82 (Y)
2	4.38 (X)	6.98 (X)	6.98 (X)
3	1.68 (T)	1.95 (Y)	1.95 (Y)
4	1.55 (Y)	1.68 (T)	1.68 (T)
5	1.07 (X)	1.39 (X)	1.39 (X)
6	0.67 (Y)	0.78 (Y)	0.78 (Y)
7	0.65 (T)	0.65 (T)	0.65 (T)
8	0.46 (X)	0.52 (X)	0.52 (X)
9	0.40 (T)	0.42 (Y)	0.42 (Y)

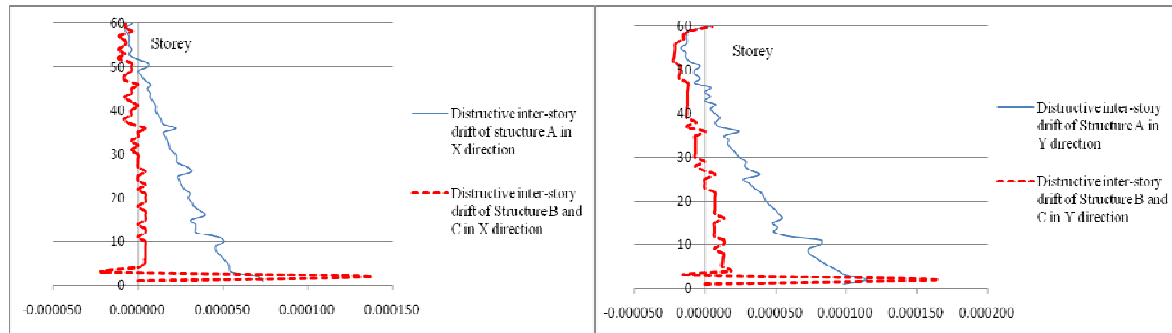
3. RESPONSE SPECTRUM ANALYSIS

The inter-story drifts of Structure A, B and C acquired by the means of response spectrum analysis is shown in Fig. 6. It is found that the inter-story drift of Structure A meet the code limitation of 1/519 specified by *Technical Specification for Concrete Structures of Tall Building* (Ministry of Housing and Urban Rural Development. 2010). The total drifts of Structure B and C are the same in both directions, which could be explained the viscous dampers of Structure C do not work under minor earthquake.

If the “harmless” drift caused by rotation of the rigid system is excluded, the inter-story drifts of Structure A, B and C is given in Fig. 7. Fig. 7 shows that the destructive inter-story drifts of the two rocking walls are very small except that at the bottom. That is to say, the structural members could be effectively protected with the deformation focusing on the rocking story.



(a). *X* direction (b). *Y* direction
Figure 6. Inter-story drifts of Structure A, B and C



(a). *X* direction (b). *Y* direction
Figure 7. "Destructive" inter-story drifts of Structure A, B and C

4. TIME HISTORY ANALYSIS

4.1. Selection of ground motions

In Chinese code, based on the site and soil classification, the requirement for the selection of ground motions is 1) the average response spectrum of the selected ground motions should be statistically match the design response spectrum; and 2) the structural base shear force of each time history analysis should be in the range of 65%~135% of that of the response spectrum analysis, and the average base shear force of all time history analysis should be 80%~120% of that of the response spectrum analysis.

Two natural earthquake records, 1940 El Centro wave and 1952 Taft wave, and one artificial wave named Rd-jwal wave were chosen for the time history analysis. The response spectra are shown in Fig. 8 and the base shears are listed in Table 3, which meets the code specifications.

Table 3. Base shear force

Ground motion	Base shear force of THA (kN)		Base shear force of RSA (kN)		Ratio of base shear force of THA to RSA	
	<i>X</i> direction	<i>Y</i> direction	<i>X</i> direction	<i>Y</i> direction	<i>X</i> direction	<i>Y</i> direction
El Centro	31970	22130	27810	22160	1.15	0.99
Taft	19300	17780			0.69	0.80
Rd-jwal	31530	24610			1.13	1.11
Average	27600	21507			0.99	0.97

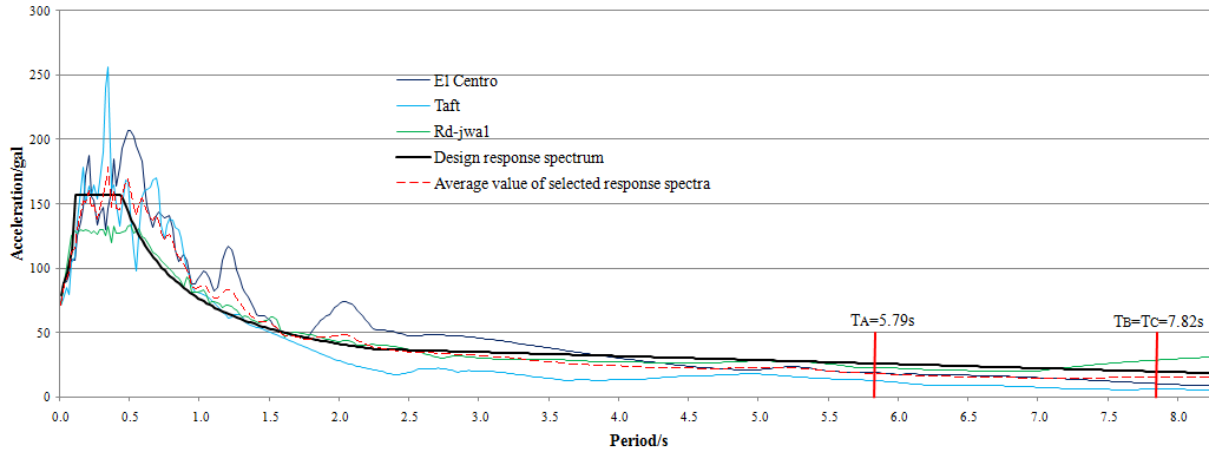


Figure 8. Response spectra of the selected ground motions and design response spectra

4.2. Inter-story drift

The peak ground accelerations of each ground motion was scaled to 0.07g, 0.20g, and 0.40g corresponding to minor, moderate, and major earthquake level, respectively. The inter-story drift results of the time history analysis and their destructive part are listed in Table 4. Results show that the inter-story drift of the structure B and C are greater than that of the structure A, but as mentioned above the inter-story drift of the rocking system consist of a part of “harmless” inter-story drift. If this part of harmless drift is removed, the destructive part of the inter-story drift of the number i^{th} floor of the structure A can be written as:

$$\bar{\theta}_i = \theta_i - \theta_{i-1} \quad (4.1)$$

where θ_i is the inter-story drift of the number i^{th} floor and θ_{i-1} is that of the number $(i-1)^{th}$ floor. The Eqn. 4.1 is transformed as,

$$\Delta u_i = \Delta \tilde{u}_i + \theta_{i-1} h_i \quad (4.2)$$

In Eqn. 4.2, Δu_i is the nominal story drift and $\Delta \tilde{u}_i$ is the destructive story drift, h_i is the storey height as shown in Fig. 9(a).

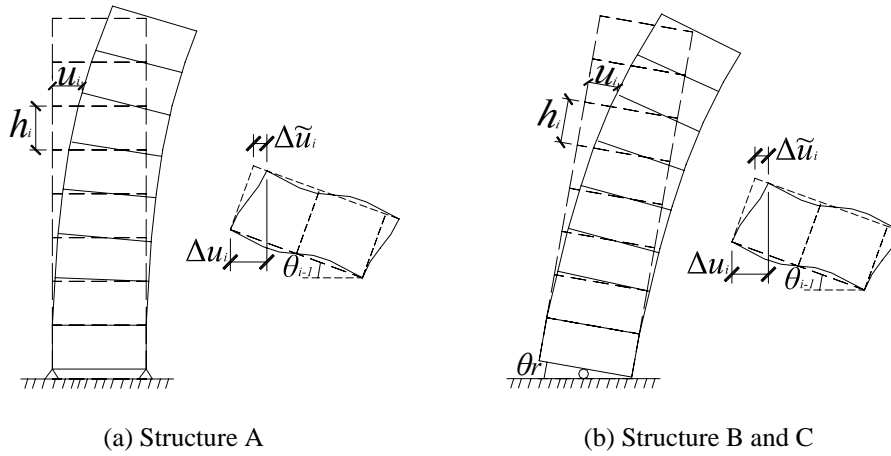


Figure 9. Inter-story drift components

As for the inter-story drift of the structural B and C, the destructive part of the inter-story drift of the

number i^{th} floor θ_{di} can be expressed in the form:

$$\theta_{di} = \bar{\theta}_i - \theta_r \quad (4.3)$$

In Eqn. 4.3, θ_r is the angle of the rigid rotation of the system as shown in Fig. 9(b).

Table 4. Inter-story drift of structures

Earthquake level	Ground motion	Structure A		Structure B		Structure C	
		X direction (Destructive part)	Y direction (Destructive part)	X direction (Destructive part)	Y direction (Destructive part)	X direction (Destructive part)	Y direction (Destructive part)
Minor earthquake	El Centro	1/787 (1/13368)	1/631 (1/9565)	1/688 (1/48288)	1/587 (1/85809)	1/729 (1/50248)	1/611 (1/89112)
	Taft	1/1498 (1/22404)	1/978 (1/18961)	1/1634 (1/98665)	1/1431 (1/15105)	1/1752 (1/109030)	1/1515 (1/194273)
	Rd-jwal	1/739 (1/13351)	1/562 (1/8372)	1/565 (1/37552)	1/328 (1/35969)	1/592 (1/36658)	1/337 (1/39886)
Moderate earthquake	El Centro	1/276 (1/4679)	1/221 (1/3349)	1/241 (1/16206)	1/205 (1/27618)	1/247 (1/17551)	1/208 (1/33329)
	Taft	1/524 (1/7841)	1/342 (1/6636)	1/572 (1/33962)	1/501 (1/58381)	1/590 (1/36361)	1/516 (1/60385)
	Rd-jwal	1/259 (1/4673)	1/197 (1/2931)	1/198 (1/11999)	1/115 (1/29685)	1/201 (1/13129)	1/116 (1/10821)
Major earthquake	El Centro	1/138 (1/2344)	1/110 (1/1679)	1/120 (1/7277)	1/103 (1/16246)	1/122 (1/8031)	1/103 (1/20955)
	Taft	1/262 (1/3920)	1/171 (1/3318)	1/286 (1/17578)	1/250 (1/34510)	1/291 (1/16135)	1/255 (1/33175)
	Rd-jwal	1/129 (1/2337)	1/98 (1/1465)	1/99 (1/7938)	1/57 (1/7976)	1/100 (1/8278)	1/58 (1/4643)

4.3. Vibration duration

A point at the roof floor was chosen to compare the difference in the vibration duration of three structures. Fig. 10 shows the displacement time history of the roof point when the El Centro wave was input. Table 5 lists the vibration duration of each structure. The analytical results show that under the same earthquake action, the vibration duration of the rocking system B is longer than that of the traditional system A. However, the existence of dampers could shorten the vibration duration of rocking structure C approximately to the traditional structure.

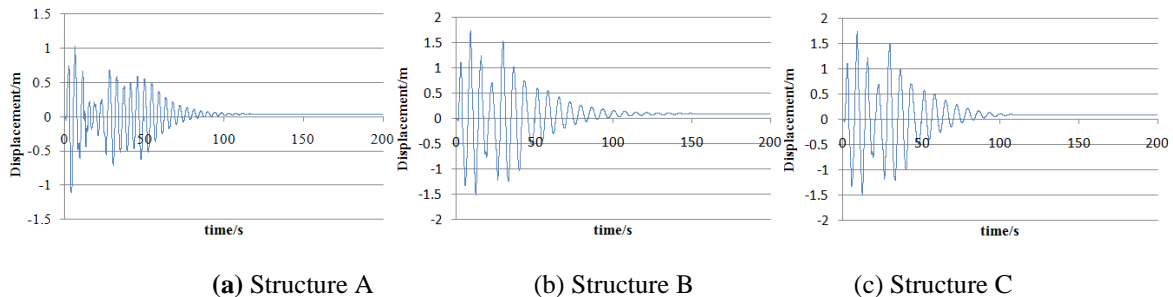


Figure 10. Displacement time history of the roof point under El Centro wave (X direction)

Table 5. Vibration duration of each structure under earthquakes

Earthquake level	Ground motion	Vibration duration <i>X</i> direction (s)			Vibration duration <i>Y</i> direction (s)		
		Structure A	Structure B	Structure C	Structure A	Structure B	Structure C
Minor earthquake	El Centro	130	150	106	132	162	122
	Taft	140	200	142	152	200	154
	Rd-jwa1	120	150	98	124	174	135
Moderate earthquake	El Centro	130	159	100	138	159	118
	Taft	143	178	158	143	200	160
	Rd-jwa1	130	160	114	138	158	118
Major earthquake	El Centro	125	158	105	139	158	120
	Taft	140	178	118	150	200	153
	Rd-jwa1	104	160	117	138	157	125

4.4. Overturning moment

The overturning moment of the three systems and that undertook by the frames are given in Table 6. Compared to the Structure A, the overturning moment shared by frames of structure B and C is increased from 20% to 59% in *X* direction and 35% to 71% in *Y* direction.

Table 6. Structural overturning moment and that undertook by frames

	Structure A		Structure B		Structure C	
	<i>X</i> direction	<i>Y</i> direction	<i>X</i> direction	<i>Y</i> direction	<i>X</i> direction	<i>Y</i> direction
Structural overturning moment (10^6 kN·m)	3.08	2.63	2.81	2.81	2.81	2.81
Overturning moment undertook by frames (10^6 kN·m)	0.64	0.94	1.68	2.02	1.68	2.02
Percentage of the overturning moment undertook by frames	20%	35%	59%	71%	59%	71%

4.5. Compressive stress of the core wall

The bottom floor core wall compressive stress is shown in Table 7. The analytical result shows that core wall compressive stress of Structure B and C could be effectively reduced by 30% compared with the traditional system A. However, the stress is still beyond the compressive strength of the concrete.

Table 7. Core wall compressive stress of the bottom core wall

Earthquake level	Structure A	Structure B	Structure C
Minor earthquake	10.98 MPa	7.68 MPa	7.29 MPa
Moderate earthquake	31.36 MPa	21.93 MPa	21.52 MPa
Major earthquake	62.72 MPa	43.86 MPa	43.44 MPa

4.6. Energy dissipation of the damper in Structure C

Two dampers are selected (Fig. 11) to check the working condition of the dampers under earthquake actions. Fig. 12~14 shows the hysteretic curves of the two dampers under three earthquake scenarios. Setting vertically, the dampers started to dissipate the energy under minor earthquakes and reached the ultimate damping forces under moderate earthquakes.

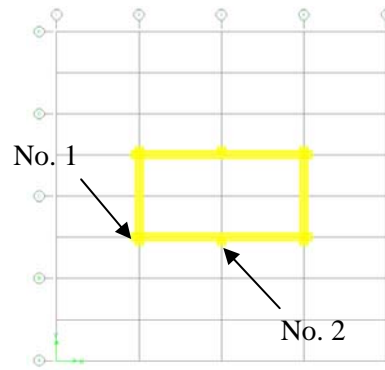
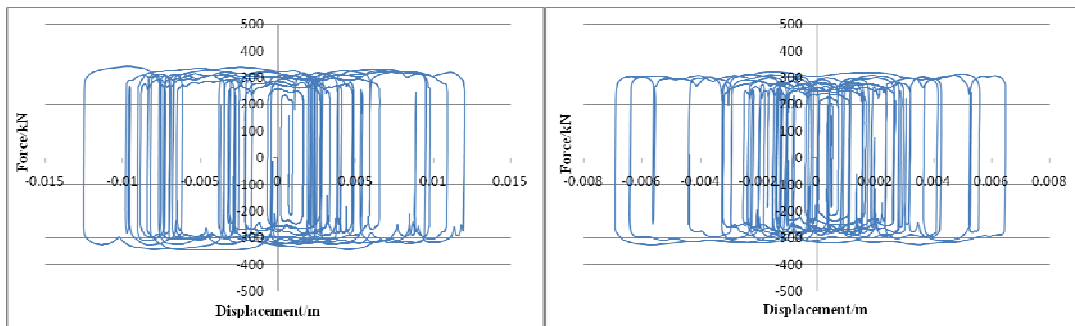


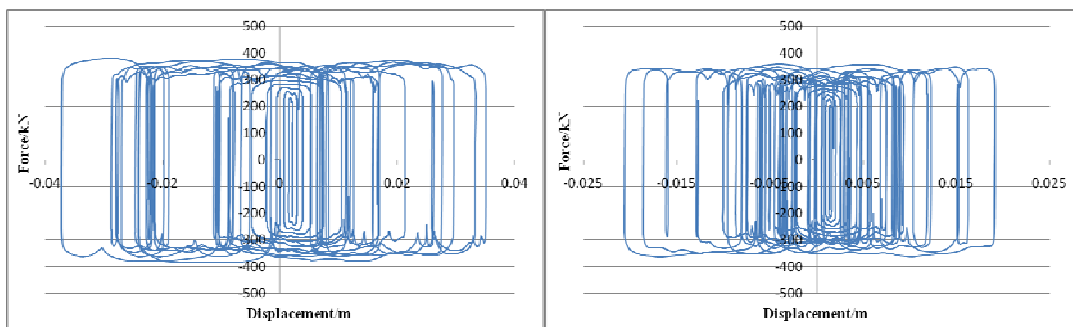
Figure 11. Location of No.1 and No. 2 damper



(a) No. 1 damper

(b) No. 2 damper

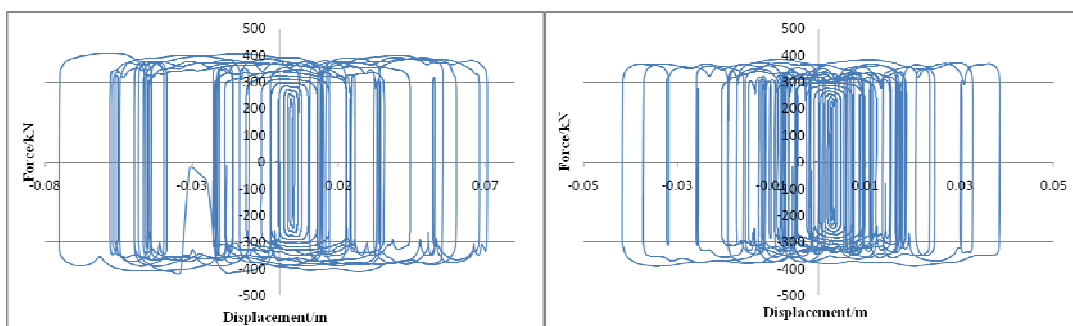
Figure 12. The hysteretic curves of two dampers under minor earthquake scenario



(a) No. 1 damper

(b) No. 2 damper

Figure 13. The hysteretic curves of two dampers under moderate earthquake scenario



(a) No. 1 damper

(b) No. 2 damper

Figure 14. The hysteretic curves of two dampers under major earthquake scenario

5. CONCLUSIONS

Earthquake resilience of tall and super-tall buildings could be realized through rocking structures, self-centering structures, replaceable structural members, etc. In this paper, rocking walls were introduced to a 240-meter-high tall building. The structural system is composed of central reinforced concrete (RC) core walls and peripheral steel reinforced concrete (SRC) frames. Three structures were analytically compared including one with traditional walls, one with rocking walls, and one with rocking walls and additional viscous dampers. Through time history analysis, it is found that for the latter two rocking systems, the fundamental period is increased by 2 s and the inter-story drift is increased by 30%. The walls are uplifted while the wall compressive stress could be effectively reduced by 30%. It is also noted that, compared to the traditional structure, the bending moment shared by frames of two rocking structures is at least increased by 30%. The existence of viscous dampers does not affect the internal forces but shorten the vibration duration approximate to the traditional structure. As a new structural earthquake-resilient system, further studies on global/local deformation and limitations, additional damping ratio, and structural details are still needed for the application of rocking walls in tall buildings.

ACKNOWLEDGEMENT

The authors acknowledge support from the National Natural Science Foundation of China (Grant No. 51078274, 51021140006), Shanghai Research Innovation Project (Grant No. 12ZZ036), and Fundamental Research Funds for The Central Universities.

REFERENCES

- Hitaka, T. and Sakino, K. (2008). Cyclic tests on a hybrid coupled wall utilizing a rocking mechanism. *Earthquake Engineering and Structural Dynamics* **37**:14,1657-1676.
- Housener, G.W. (1963). The behavior of inverted pendulum structures during earthquakes. *Bulletin of the Seismological Society of America* **53**:2,403-417.
- Hukelbridge, A.A. (1977). Earthquake simulation tests of a nine story steel frame with columns allowed to uplift. Report No. UCB/EERC-77/23. Berkely: University of California, Berkely.
- Hukelbridge, A.A. and Clough, R.W. (1977). Preliminary experimental study of seismic uplift of a steel frame. Report No. UCB/EERC-77/22. Berkely: University of California, Berkely.
- Kurama, Y.C. (2000). Seismic design of unbonded post-tensioned precast concrete walls with supplemental viscous damping. *ACI Structural Journal* **97**:4,648-658.
- Nielsen, G.M., Almufti, I., and Mahin, S.A., et al. (2010). Performance of rocking core walls in tall buildings under sever seismic motions. *Proceedings of the 9th US National and 10th Canadian Conference on Earthquake Engineering*, Paper No. 483. Ottawa, Canada.
- Ministry of Housing and Urban Urual Development. (2010). *Technical Specification for Concrete Structures of Tall Building* (JGJ3-2010). Beijing: China Architecture & Building Press.
- PEER. (2010). Report of the seventh joint planning meeting of NEES/E-defense collaborative research on earthquake engineering. Pacific Earthquake Engineering Research Center, Berkeley: Unibersity of California, Berkeley.
- Priestly, M.J.N, Evison, R.J. and Carr, A.J. (1978). Seismic response of structures free to rock on their foundations. *Bulletin of the New Zealand National Society for Earthquake Engineering* **11**:3,141-150.
- Zhou, Y. and Lu, X.L. (2011). State of the art on rocking and self-centering structures. *Journal of Building Structures* **32**:9,1-10. (in Chinese)